Carbohydrate Polymers 118 (2015) 126–132

Contents lists available at ScienceDirect

Carbohydrate Polymers

journal homepage: www.elsevier.com/locate/carbpol

Preparation of bulk sodium carboxymethyl cellulose aerogels with tunable morphology

Runjun Lin, Ang Li, Lingbin Lu*, Yang Cao

Key Lab of Advanced Materials of Tropical Island Resources, Ministry of Education, College of Materials and Chemical Engineering, Hainan University, No. 58, Renmin Avenue, Haikou 570228, Hainan, China

ARTICLE INFO

Article history:
Received 2 September 2014
Received in revised form 24 October 2014
Accepted 28 October 2014
Available online 20 November 2014

Keywords:
CMC aerogel
Iron ion
Tunable morphology
Coordination

ABSTRACT

Homogeneous and bulk carboxymethyl cellulose hydrogel and aerogel were prepared by a novel process, using Fe^{3+} and D-(+)-gluconic acid-lactone as cross-linker and releasing agent, respectively. The results showed that the mass fraction of Fe^{3+} has a great effect on CMC aerogels' structure, crystallization and morphology. By adjusting the mass fraction of Fe^{3+}, granular, three-dimensional network and rod-like morphology were obtained, responding to varying density and porosity. The aerogel had low density (low to 0.0568 g/cm^3) and high porosity (up to 90.45%). Meantime. Combination patterns between carboxylate ion and iron ion were checked by FTIR. Furthermore, with the addition of Fe^{3+}, lattice mismatch of CMC emerged and led to decreasing crystalline degree and thermal stability. This work would play an important role in the handy and extensive application of CMC aerogels

1. Introduction

Cellulose is the most abundant natural polysaccharide on the earth, which is renewable, sustainable, as well as eco-friendly. It has been developed for hundreds of years and wildly applied in various areas. However, its insolubility leads to numerous obstacles and limitation in the processing and application. Its water-soluble derivatives gained more attention instead. Herein, sodium carboxymethyl cellulose (CMC) is one of the most common derivates formed by the carboxymethylation of the hydroxyl group of cellulose. Due to its solubility, biocompatibility and biodegradation, CMC is utilized in scaffolds (Ko, Sfeir, & Kumta, 2010), agriculture (Davidson, Verma, & Gu, 2013; Puoci et al., 2008), stabilizers (He & Zhao, 2007), barriers (Jabbour, Bongiovanni, Chaussy, Gerbaldi, & Beneventi, 2013; Wang & Wang, 2014; Qiu et al., 2014) and medication (Buzzi et al., 2013; Kaihara, Suzuki, & Fujimoto, 2010; Sannino et al., 2003a; Sannino, Maffezzoli, & Nicolais, 2003b), etc. extensively.

While, few reports can be found about solely CMC aerogels and most of them were halted at the hydrogels. Furthermore, CMC is usually utilized as a binder in composites, with other materials as strong backbone or skeleton, such as CMC-alginate (Cheng, Lu, Zhang, Shi, & Cao, 2012), CMC-chitosan (Chen, Liu, Feng, & Shao, 2005), CMC-cellulose (Olszewska et al., 2013; Chang, Duan, Cai, & Zhang, 2010), CMC-PEG (Sannino et al., 2003a,b), CMC-PVA (Bajpai & Giri, 2002), CMC-TiO_2 (Pasqui, Atrei, Giani, De Cagna, & Barbucci, 2011), CMC-Si (Guo & Wang, 2010), CMC-clay (Ma, Zhang, Fan, Xu, & Liang, 2008), etc. Generally, CMC hydrogels could be prepared with three common processes. One of the most common processes is that CMC was cross linked by epichlorohydrin (ECH), reported in numerous literatures (Chang et al., 2010; Adel, Abou Youssef, El Gendy, & Nada, 2010). The second, CMC hydrogel is obtained with glutaraldehyde as cross-linker at a special temperature and pH (Devi & Maji, 2009) by emulsion method (Rokhade, Kulkarni, Mallikarjuna, & Aminabhavi, 2009; Sullad, Manjeshwar, & Aminabhavi, 2011; Ramesh, Sairam, & Hosamani, 2007), which has been widely applied in drug delivery aera. The third one is that CMC is cross linked with metal ions (Nie, Liu, Zhan, & Guo, 2004; Li et al., 2013; Nadagouda & Varma, 2007), such as Ca^{2+}, Mg^{2+}, Al^{3+} and Fe^{3+}. Compared with the former two methods, the third process was not only facile and quick, but also non-toxic and eco-friendly, for ECH and glutaraldehyde was either poisonous or inert. Meantime, the third method also has a few defects and inconveniences, for its uneven dispersion and uncontrollable coordination rate of metal ions. Hence, CMC micro spheres, beads (Bourlinos & Petridis, 2002) and films were usually prepared by this method yet bulk hydrogels were barely obtained. Besides, the metal ions' concentration also has an immense impact on CMC aerogels' structure.

In this manuscript, bulk CMC aerogels were obtained via a facile and novel method. In order to achieve a homogeneous structure,

* Corresponding author. Tel.: +86 0898 66290799; fax: +86 0898 66279219.
E-mail address: lulingbin@126.com (L. Lu).

http://dx.doi.org/10.1016/j.carbpol.2014.10.075
0144-8617/

Table 1
Systematical mixture ratio of the preparation of CMC aerogels.

mr*	m(CMC)/g			m(GDL)/g			m($FeCl_3·6H_2O$)/g			Density/g/cm^3			Porosity/%		
	3%	5%	7%	3%	5%	7%	3%	5%	7%	3%	5%	7%	3%	5%	7%
0.294 (mr1)	3	5	7	1.74	2.90	4.06	0.882	1.470	2.058	0.0609	0.0963	0.1423	77.4	73.6	59.7
0.588 (mr2)	3	5	7	1.74	2.90	4.06	1.764	2.940	4.117	0.0568	0.0800	0.1274	90.5	84.0	77.3
0.882 (mr3)	3	5	7	1.74	2.90	4.06	2.646	4.411	6.175	0.0696	0.1079	0.1560	89.5	81.6	73.3
1.176 (mr4)	3	5	7	1.74	2.90	4.06	3.528	5.881	8.233	0.0722	0.1175	0.1680	87.9	80.5	76.7
1.470 (mr5)	3	5	7	1.74	2.90	4.06	4.411	7.351	10.291	0.0777	0.1158	0.1847	83.3	79.8	75.6

Note: mr* means the weight ratio of $FeCl_3·H_2O$/CMC.

$Fe^{3+}$and D-gluconic acid-δ-lactone (GDL) was utilized as crosslinking agent and releasing agent, respectively. And we focus on the effect of Fe^{3+} concentration on the aerogels' physicochemical properties and micromorphology. Aerogels' thermal stability, crystallization behavior and adsorbency were also investigated.

2. Experimental

2.1. Materials

Sodium carboxyl methyl cellulose (CMC) was obtained from Tianjin FuChen Chemical Reagents Factory and used as received. The mass fraction of sodium content ranged from 6.5% and 8.5%. $FeCl_3·6H_2O$ (AR), D-(+)-gluconic acid-lactone (99%) and ammonia solution (25%) was purchased from Guangzhou Xilong Chemical Co., Ltd., Aladdin Reagents Co., Ltd. and Guangzhou Chemical Reagent Factory, and all chemical reagents were used without further purification, deionized water was used for experiments unless otherwise mentioned.

2.2. Preparation of bulk CMC aerogels

In the first step, CMC and GDL (Constant weight ratio of GDL/CMC was equal to 0.588) were co-dispersed in water homogeneously, and five batches of $FeCl_3·6H_2O$ (the weight ratio of $FeCl_3·6H_2O$/CMC equivalent to 0.294, 0.588, 0.882, 1.176 and 1.470.) were dissolved in deionized water followed by adjusting the solutions pH equal to ca. 7 with ammonia solutions. The samples were labeled as mr1, mr2, mr3, mr4 and mr5, respectively (Table 1). Then the solution was combined with CMC solution and injected in a mould. Gelation of the sol has occurred in a few hours. The gel was kept for three days for a more complete gel structure at room temperature. The hydrogel was rinsed with deionized water repeatedly. Finally, bulk CMC aerogels were obtained through lyophilization (LGJ-18A lyophilizer, Four-Ring Science Instrument Plant Beijing Co., Ltd). Methods of preparing other mass fraction of CMC aerogels were the same as above.

2.3. Estimation of density and porosity

The regular cylindrical aerogels were dried, weighted and recorded as m_0. The volume of aerogel cylinder was calculated as Eq. (1). (Herein, D means diameter of aerogels, measured by a caliper for 3 times and taken the average value), recording as V. The density (ρ) was calculated by Eq. (2). At the same time, the aerogel sample (m_1) was put in a container, filling with ethanol. And the aerogel was soaking for one hour until no bubble spilled out of the sample. Took out the sample and weighted it, recorded as m_2. Thereby, porosity of the aerogel sample was calculated according to Eq. (3).

$$V = \frac{4}{3}\pi\left(\frac{D}{2}\right)^2 \times h \quad (1)$$

$$\rho = \frac{m_0}{V} \quad (2)$$

$$\delta = \frac{m_2 - m_1}{m_2} \times 100\% \quad (3)$$

3. Results and discussion

3.1. Optimal process

Density and porosity are the essential performance of aerogels, which have vital effects on aerogels' properties and applications. In Table 1, density and porosity of aerogels with different mixture ratios were included. With the weight ratio of $FeCl_3·6H_2O$/CMC increasing, the aerogel's density increased after slightly declined. The minimum density was obtained from the ratio equal to 0.588 (mr2). On the contrary, in terms of porosity, after slightly increased, the variance of porosity almost flattened. The minimum density and maximum porosity were 0.0568 g/cm^3 and 90.45%, respectively. Hence, the optimal process is right on mr2 and 3%CMC. These trends reflected the structure's differences, which will be discussed later.

3.2. FTIR analysis

In order to understand the bond behavior between Fe^{3+} and R-COO^-, FT-IR was utilized. Infrared spectroscopy of CMC aerogels (the mass fraction of CMC is 3%) was shown in Fig. 1. In raw CMC, the strong and broad absorption peak at 3445.45 cm^{-1} was the stretching frequency of the —OH group as well as intra- and inter-molecular hydrogen bonds. Because there were many strong polar hydroxyl groups in CMC molecular, which were easy to form hydrogen bonds with another electron donating groups, such as —OH and C—O—C. The band at 1326.14 cm^{-1} was assigned to —OH bending vibration. There were also two visible absorption bands at 1616.78 cm^{-1} and 1419.73 cm^{-1}, which were assigned to carboxylate characteristically. The former was due to asymmetry stretching vibration peak of —COO—, while the latter was attributed to its symmetry vibration. Affected by the ring tension of six-membered in CMC, the bands at 2924.74 cm^{-1} and 618.27 cm^{-1} were due to C-H stretching vibration and bending vibration in plane, respectively (Cheng et al., 2012). The existence of ether linkage of glycoside bond and cyclic ether linkage of six-membered rings proved by the absorption band at 1119.68 cm^{-1} due to the asymmetry stretching vibration peak of C—O—C.

Comparing with the FTIR spectra of raw CMC, there were only slight changes of the absorbency peaks of CMC aerogels. The absorption bands of carboxylate were gradually shifted, proving that the cloud density was changed by the existence of Fe^{3+}. Shape of the $\upsilon_a\left(CO_2^-\right)$ band of the Fe-CMC was distinctly narrower and sharper compared to the same type of bands of the CMC spectra. It could be linked with orthodox coordination spheres. According to previous study (Nakamoto, 1978; Fuks, Filipiuk, & Majdan, 2006), there were mainly three combination patterns for carboxylate ion and a metal as shown in Fig. 2 (Nakamoto, 1978), including unidentate complex (structure I), chelating complex (structure II) and bridging complex (structure III). It would be unidentate complex when Δ value $[\upsilon_a\left(CO_2^-\right) - \upsilon_s\left(CO_2^-\right)]$ was much greater than

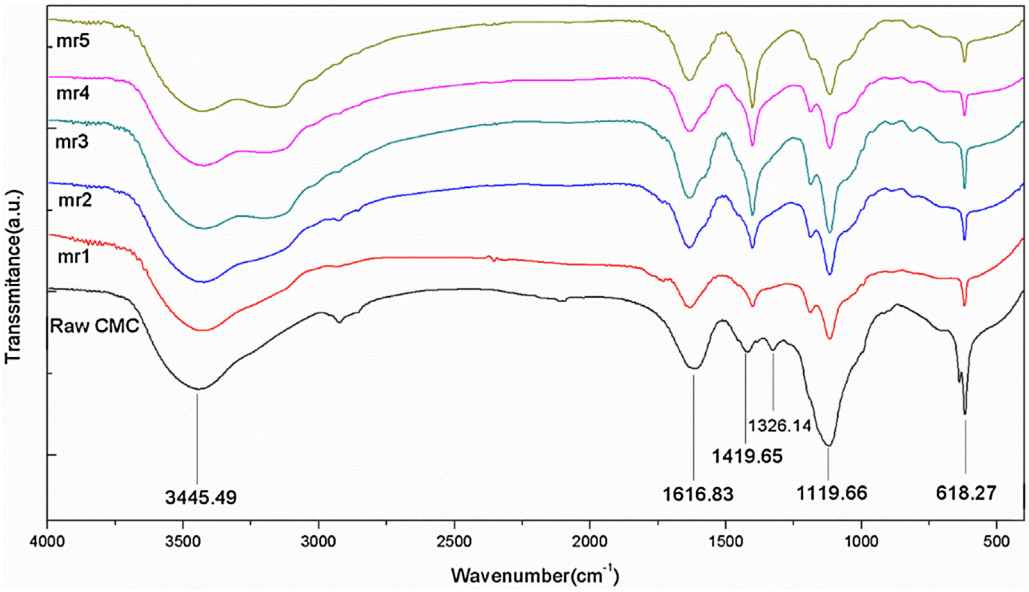

Fig. 1. FTIR spectra of 3% CMC aerogels with various $FeCl_3{\cdot}6H_2O$/CMC weight ratios.

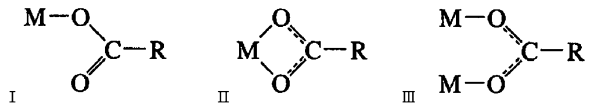

Fig. 2. Three coordination patterns of carboxylate ion and metal ion (I, Unidentate complex; II, Chelating complex; III, Bridging complex).

the ionic complex (e.g. CMC-Na). Chelating complex could be got if Δ value was much more less. The Δ value for bridging complex was greater than those of chelating complex, and close to the ionic value. According this spectra, Δ values of $[\upsilon_a(CO_2^-) - \upsilon_s(CO_2^-)]$ were listed in Table 2, and it could be obviously concluded that the pattern of CMC aerogel was unidentate complex.

Besides, the stretching vibration absorbency peaks of C—O were slightly shifted to low wavenumber for 3 cm^{-1}. The bending vibration absorbency intensity of C-H was also decreased critically. These illustrated that the intensity of intermolecular hydrogen bands increased visibly, leading to the molecular interaction grow strong in CMC aerogels. Furthermore, because of the existence of Fe^{3+}, electron cloud density of carboxylate ions was decreased after gelation. It resulted in weak repulsive force among carboxylate ions and short molecular distances. It was the major cause of increasing hydrogen bands (De Britto & Assis, 2009). The bands absorbency at 1326 cm^{-1} shifted to high wavenumber (about 139 cm^{-1}) after gelation. It indicated that the bending vibration of —OH was inhibited by strong hydrogen bands. Meantime, weak repulsive force also made C=O vibrate more freely, which can be proved by the blue shift of C=O stretching vibration (about 20 cm^{-1}) as well.

Table 2
Δ Values and the combination patterns between carboxylate ion and iron ion in CMC aerogel.

Samples	υ_a (COO)[a]	υ_s (COO)[a]	Δ	Structure
CMC-Na	1616.83	1419.65	197.18	Ionic
CMC-Fe mr1	1632.48	1400.85	231.63	Unidentate
CMC-Fe mr2	1635.45	1401.18	234.27	Unidentate
CMC-Fe mr3	1636.06	1401.09	234.97	Unidentate
CMC-Fe mr4	1633.66	1401.13	232.53	Unidentate
CMC-Fe mr5	1635.07	1401.35	233.72	Unidentate

[a] These correspond to the υ(C=O) (free) and υ(C—O) (coordinated) of the unidentate carboxylates, respectively.

3.3. Morphology analysis

Morphology of 3%CMC aerogels with different $FeCl_3{\cdot}6H_2O$/CMC weight ratios were characterized by SEM with an acceleration voltage of 5 kV (Fig. 3). From the pictures, granular, three-dimensional network and rod-like morphology were observed with increasing weight ratio of Fe^{3+}. With low weight ratio of Fe^{3+}, there were more coordinate bonds between Fe^{3+} and carboxylate ion. Each iron ion possibly coordinated by almost six carboxylate ions, as depicted in Fig. 4(a). The d layer electron distribution of iron ions is spherically symmetric with high spin, which tends to form sphere particles during the process of coordination. The shape of the $\upsilon_s(CO_2^-)$ band of the Fe-CMC was distinctly narrower and sharper compared to the same type of band in the CMC FTIR spectra. It could be linked with orthodox coordination spheres[32]. These all resulted in a granular morphology (Fig. 3 mr1). Besides, homogeneous granular particles piled up compactly. It led to a high density and low porosity structure, which were corresponding to the experimental data. Krishna et al. (2006) ever reported this phenomenon, only they did not notice the morphology changes with various metal ion concentration. While, for mr2, three-dimensional network was observed. Lamellar structure was also observed at a lower resolution. It indicated that CMC molecule was linked by different iron ions, which was good for the forming of three-dimensional network. The 3-D structure was formed with the support of iron ions, depicting in Fig. 4(b). It made a great attribution to increase porosity and decrease density. Meantime, a few granular particles were adhered to the 3-D structure. It might be formed by the bands between iron ion and residues, like residual Cl^- and $C_5O_5H_{11}COO^-$ (GDL's hydrolysate). Energy dispersive spectroscopy of mr2 aerogel also illustrated this phenomena with the peak of Cl. However, with the increasing weight ratio of Fe^{3+}, too many iron ions around CMC molecule, and the bridging function of iron ions did not give full play. Hence, rod-like structure was observed, depicting in Fig. 4(c).

3.4. Thermal stability

In order to understand the thermal stability of CMC aerogels, TG and DTG were conducted at 10 °C/min, with raw CMC as reference. And the thermograms were shown in Fig. 5. From the raw CMC curve, a small peak at 51 °C was observed in response to loss

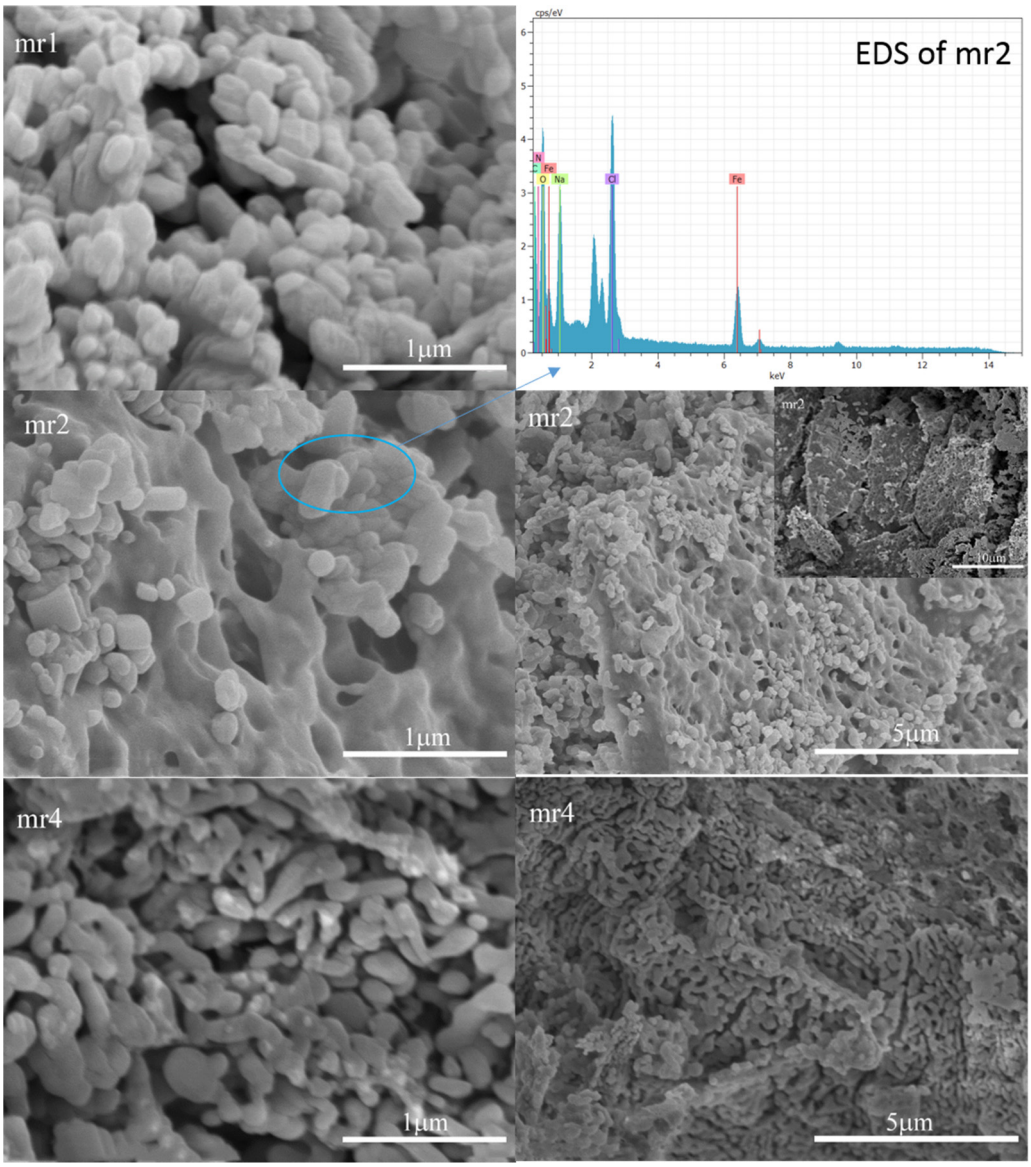

Fig. 3. SEM pictures for CMC (3%) aerogels; the right is of high resolution(×40 k) and the left is lower(×10 k); the left top graph is energy dispersive spectroscopy of mr2.

of adsorbed water. And a sharp decline from 240 °C to 330 °C was attributed to the loss of hydroxyl groups. With increasing temperature to 675 °C, carboxyl groups began pyrolysis. Compared with raw CMC, mr2 aerogel had a similar thermal events generally. There was an extra peak at around 200 °C, which could be due led to by impurities, like residual GDL. Thermal stability of CMC was weakened with the addition of Fe^{3+} due to the synergistic effect and a larger radius of ion ions than sodium ions, as reported in other literatures (Lombardi & Mercê, 2003; Prasad & Kalyanasundaram, 1994; Nimlos, Blanksby, Ellison, & Evans, 2003)

3.5. Crystalline phase analysis

In order to explore the phase variation of CMC aerogels, X-ray diffractometry (λ = 1.54184) was also utilized. The diffraction angle ranged from 4 to 45°. As showed in Fig. 6, phase changes of raw CMC

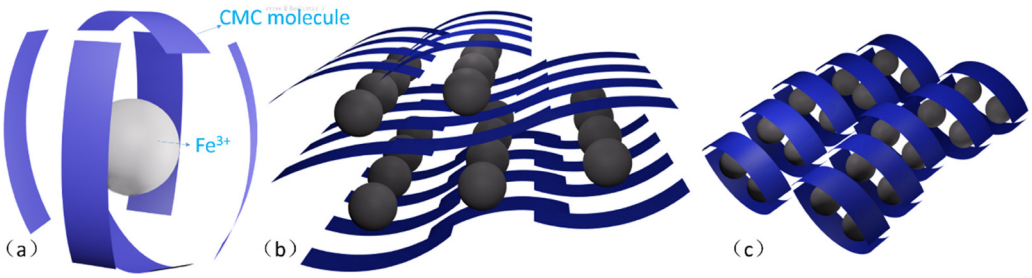

Fig. 4. Structure models for the coordination patterns of CMC and Fe^{3+}.

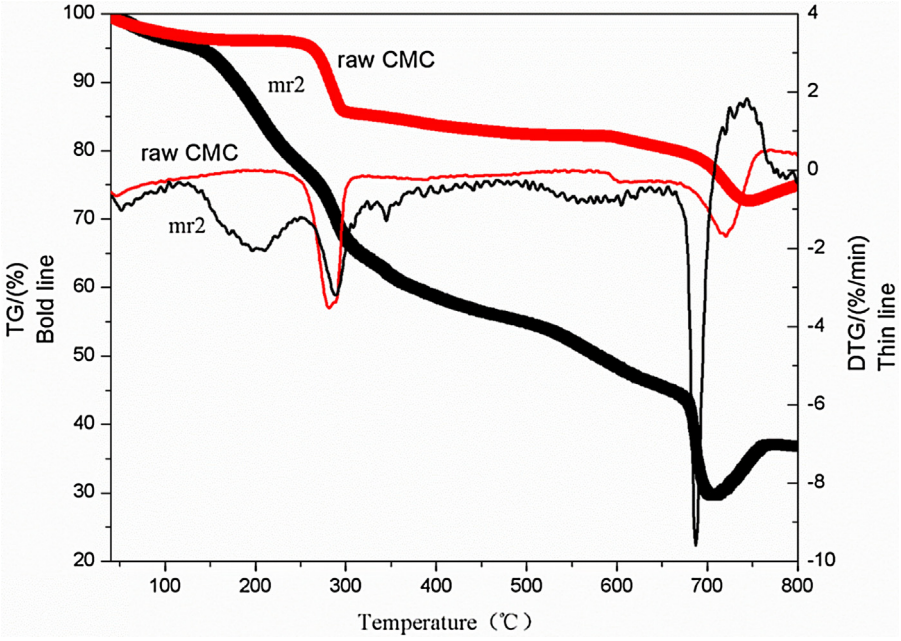

Fig. 5. TG and DTG curve of raw CMC and mr2 CMC aerogel.

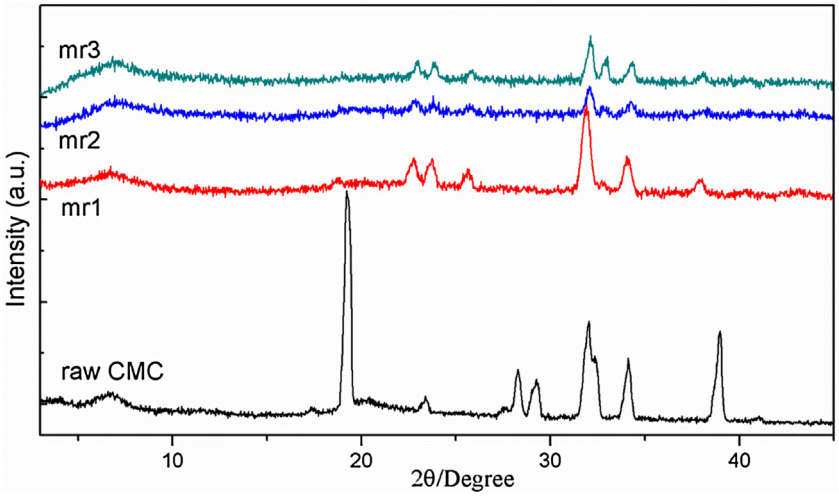

Fig. 6. X-ray diffractometry profiles of CMC raw material and 3% CMC aerogels.

material and CMC aerogels with various Fe^{3+} mass fraction were depicted. The degree of crystallinity (χ_c) was calculated according to the usual method (Rabek, 1980), presented in Table 3. The raw CMC was a high crystal material, with χ_c = 65.63%, which was similar to natural cellulose due to its low degree of substituent. The degree of crystallinity decreased after formed CMC aerogels. Due to its crystalline nature, raw CMC showed characteristic intense peak at 2θ of 19.48°, 28°, 29° and 39°. However, these peaks either disappeared or decreased in CMC aerogels. It noted that the crystal structure was broken with the addition of Fe^{3+}, and chelation reaction occurred between iron and carboxylate ions. It was also verified by the decreased χ_c with the increasing mass fraction of Fe^{3+}. Besides, the diffractive peak at 23.35° of raw CMC was divided into two peaks at 22.7° and 23.7° in CMC aerogels, respectively. It could be inferred that a few of iron ions permeated into CMC crystal lattice, and identity distance increased slightly due to the larger atomic radius of iron ions. It gave rise to a mild shift of diffractive angle. The increasing crystalline degree was also in accord with decreased thermal stability. With the addition of Fe^{3+}, lattice mismatch emerged and resulted in crystalline degree decreased. Hence, thermal stability of CMC aerogels decreased

Table 3
The degree of crystallinity of raw CMC and 3% CMC aerogels.

Samples	Raw CMC	mr1 CMC aerogel	mr2 CMC aerogel	mr3 CMC aerogel
Crystallinity	65.63%	51.42%	51.32%	46.40%

3.6. Absorbency

The weight ratio of $FeCl_3 \cdot H_2O$/CMC equivalent to 0.588 was optimum process, according to the variation of absorbency shown in Fig. 7. CMC aerogels with various CMC concentration at a constant weight ratio of $FeCl_3 \cdot H_2O$/CMC were synthesized. While, at the mass fraction of CMC equivalent to 2%, homogeneous gel can't be obtained owing to the low viscosity and precipitation of $Fe(OH)_3$ clusters. From Fig. 8, the density increased uninterrupted with

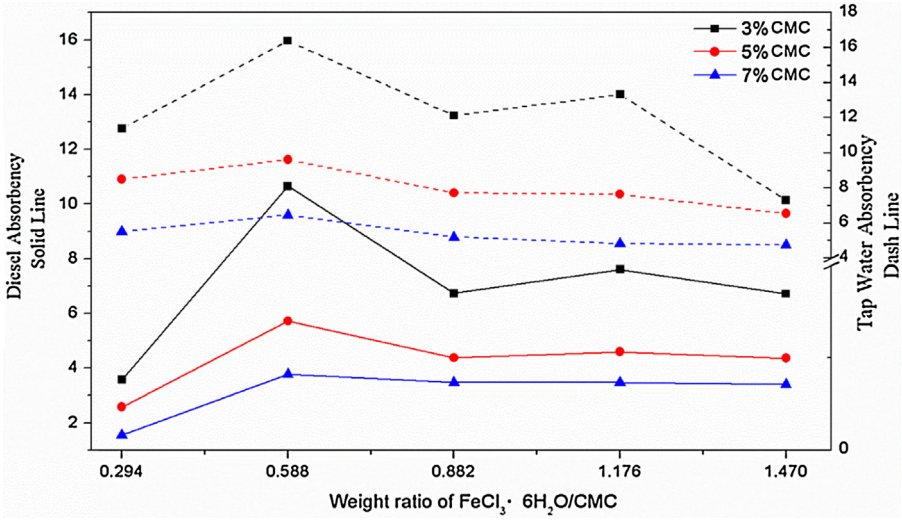

Fig. 7. Absorbency of CMC aerogel with various $FeCl_3 \cdot H_2O$/CMC weight ratios.

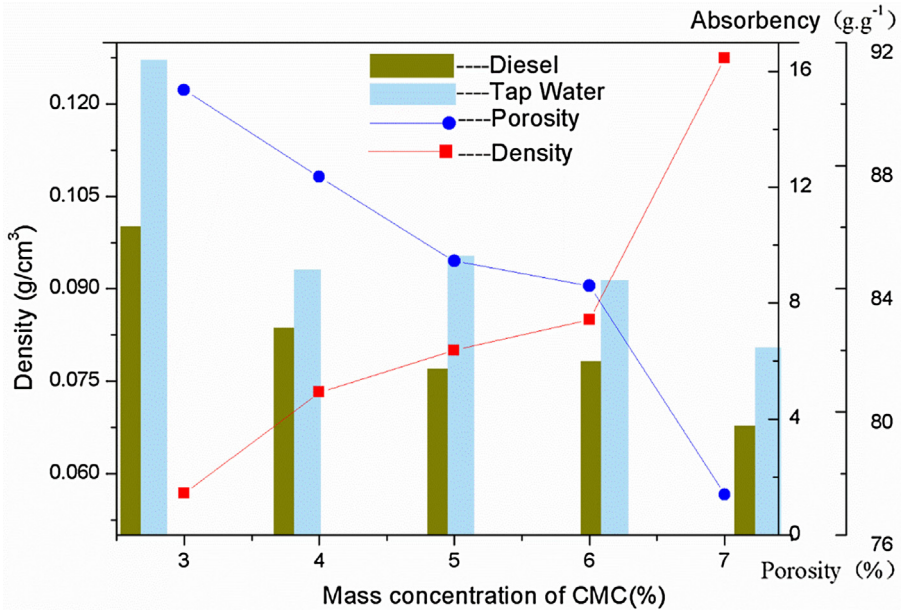

Fig. 8. Density, porosity and absorbency of CMC aerogels at constant weight ratio of $FeCl_3 \cdot H_2O$/CMC equivalent to 0.588 with different CMC concentration.

increasing CMC concentration, while the porosity exactly went to a reverse tendency. It could be explained by the formation of a rigid network at higher amounts of CMC. AP Rokhade et al. reported the similar finding (Rokhade et al., 2006). At the same time, diesel and tap water absorbency were counted as well as illustrated in Fig. 8. An identical variation tendency to porosity was observed. The maximum absorbency of diesel and tap water was 10.65 g g^{-1} and 16.39 g g^{-1}, respectively, Therefore, CMC aerogel has the potential application as pollutants absorbent. Research on the adsorption mechanism is still under further study.

4. Conclusion and perspectives

Bulk CMC aerogel with tunable morphology was synthesized by a novel method in this manuscript. The influence of Fe^{3+} on aerogels' structure was investigated. The results demonstrated that by adjusting the weight ratio of $FeCl_3 \cdot H_2O$/CMC, CMC aerogels with different morphology, including granular, three-dimensional network and rod-like morphology, could be obtained, responding to various density, porosity and absorbency. By further treatment, magnetic CMC aerogel could be achieved. It can be predicted other metal ions, such as like Al^{3+}, Cu^{2+}, Ti^{4+} and Ca^{2+}, could result in homogeneous CMC aerogels by this method as well. More new aerogels with different color, magnetic and optical properties can be expected.

Acknowledgements

The authors gratefully acknowledge financial support from the Projects of Science Foundation of Hainan Province (No. 512113), the Young Scientist Project of Hainan University (No. Qnjj1235), the Special Fund for Integrated Industry-University-Research of Hainan Province (No. Cxy20140039) and the Postgraduates Projects of Science and Technology Innovation (2014).

References

Adel, A. M., Abou Youssef, H., El Gendy, A. A., & Nada, A. M. (2010). Carboxymethylated cellulose hydrogel; sorption behavior and characterization. *Nature Science*, *8*(8), 244–256.

Ramesh Babu, V., Sairam, M., Hosamani, K. M., & Aminabhavi, T. M. (2007). Preparation of sodium alginate–methylcellulose blend microspheres for controlled release of nifedipine. *Carbohydrate Polymer*, *69*, 241–250.

Bajpai, A. K., & Giri, A. (2002). Swelling dynamics of a macromolecular hydrophilic network and evaluation of its potential for controlled release of agrochemicals. *Reactive & Functional Polymers*, *53*, 125–141.

Bourlinos, A. B., & Petridis, D. (2002). Shape fabrication of millimeter-sized metal-containing carboxymethyl cellulose hollow capsules. *Chemical Communications*, *23*, 2788–3278.

Buzzi, V., Brudner, M., Wagner, T. M., Bazzo, G. C., Pezzin, A. P. T., & Silva, D. A. K. (2013). Caboxymetylcellulose/gelatin blends loaded with piroxicam: Preparation, characterization and evaluation of in vitro release profile. *Journal of Encapsulation and Adsorption Sciences*, *3*(4), 99–107.

Chen, X., Liu, J., Feng, Z., & Shao, Z. (2005). Macroporous chitosan/carboxymethyl cellulose blend membranes and their application for lysozyme adsorption. *Journal of Applied Polymer Science*, *96*(4), 1267–1274.

Chang, C., Duan, B., Cai, J., & Zhang, L. (2010). Superabsorbent hydrogels based on cellulose for smart swelling and controllable delivery. *European Polymer Journal*, *46*, 92–100.

Cheng, Y., Lu, L., Zhang, W., Shi, J., & Cao, Y. (2012). Reinforced low density alginate-based aerogels: Preparation, hydrophobic modification and characterization. *Carbohydrate Polymers*, *88*(3), 1093–1099.

Devi, N., & Maji, T. K. (2009). Preparation and evaluation of gelatin/sodium carboxymethyl cellulose polyelectrolyte complex microparticles for controlled delivery of isoniazid. *AAPS Pharmscitech*, *10*, 1412–1419.

De Britto, D., & Assis, O. B. (2009). Thermal degradation of carboxymethylcellulose in different salty forms. *Thermochemical ACTA*, *494*(1), 115–122.

Davidson, D. W., Verma, M. S., & Gu, F. X. (2013). Controlled root targeted delivery of fertilizer using an ionically crosslinked carboxymethyl cellulose hydrogel matrix. *Springer Plus*, *2*(1), 318.

Fuks, L., Filipiuk, D., & Majdan, M. (2006). Transition metal complexes with alginate bisorbent. *Journal of Molecular Structure*, *792*, 104–109.

Guo, J., & Wang, C. (2010). A polymer scaffold binder structure for high capacity silicon anode of lithium-ion battery. *Chemical Communications*, *46.*, 1428–1430.

He, F., & Zhao, D. (2007). Manipulating the size and dispersibility of zerovalent iron nanoparticles by use of carboxymethyl cellulose stabilizers. *Environmental Science & Technology*, *41*(17), 6216–6221.

Jabbour, L., Bongiovanni, R., Chaussy, D., Gerbaldi, C., & Beneventi, D. (2013). Cellulose-based Li-ion batteries: A review. *Cellulose*, *20*(4), 1523–1545.

Kaihara, S., Suzuki, Y., & Fujimoto, K. (2010). In situ synthesis of polysaccharide nanoparticles via polyion complex of carboxymethyl cellulose and chitosan. *Colloids and Surfaces B: Biointerfaces*, *85*(2), 343–348.

Ko, H. F., Sfeir, C., & Kumta, P. N. (2010). Novel synthesis strategies for natural polymer and composite biomaterials as potential scaffolds for tissue engineering. *Philosophical Transaction of the Royal Society A: Mathematical Physical and Engineering Sciences*, *368*, 1981–1997.

Krishna Rao, K. S. V., Subha, M. C. S., Vijaya Kumar Naidu, B., Sairam, M., Mallikarjuna, N. N., & Aminabhavi, T. M. (2006). Controlled release of diclofenac sodium and ibuprofen through beads of aodium alginate and hydroxy ethyl cellulose blends. *Journal of Applied Polymer Science*, *102*, 5708–5718.

Lombardi, S. C., & Mercê, A. L. R. (2003). Properties of complexes of galactomannan of leucaena leucocephala and Al^{3+}, Cu^{2+} and Pb^{2+}. *Bioresource Technology*, *89*(1), 63–73.

Li, L., Xiang, S., Cao, S., Zhang, J., Ouyang, G., Chen, L., et al. (2013). A synthetic route to ultralight hierarchically micro/mesoporous Al(III)-carboxylate metal-organic aerogels. *Nature Communications*, *4*, 1774–1782.

Ma, J., Zhang, L., Fan, B., Xu, Y., & Liang, B. (2008). A novel sodium carboxymethylcellulose/poly(*N*-isopropylacrylamide)/clay semi-IPN nanocomposite hydrogel with improved response rate and mechanical properties. *Journal of Polymer Science, B: Polymer Physics*, *46*, 1546–1555.

Nakamoto, K. (1978). *Infrared and Raman spectra of inorganic and coordination compounds Part B* (6th ed.). New Jersey: John Wiley & Sons, Inc. Chapter 1.

Nimlos, M. R., Blanksby, S. J., Ellison, G. B., & Evans, R. J. (2003). Enhancement of 1,2-dehydration of alcohols by alkali cations and protons: A model for dehydration of carbohydrates. *Journal of Analytical and Applied Pyrolysis*, *66*(1), 3–27.

Nie, H., Liu, M., Zhan, F., & Guo, M. (2004). Factors on the preparation of carboxymethylcellulose hydrogel and its degradation behavior in soil. *Carbohydate Polymers*, *58*, 185–189.

Nadagouda, M. N., & Varma, R. S. (2007). Synthesis of thermally stable carboxymethyl cellulose/metal biodegradable nanocomposites for potential biological applications. *Biomacromolecules*, *8*, 2762–2767.

Olszewska, A., Junka, K., Nordgren, N., Laine, J., Rutland, M. W., & Österberg, M. (2013). Non-ionic assembly of nanofibrillated cellulose and polyethylene glycol grafted carboxymethyl cellulose and the effect of aqueous lubrication in nanocomposite formation. *Soft Matter*, *9*(31), 7448–7457.

Prasad, M. P., & Kalyanasundaram, M. (1994). Thermal analysis of controlled-release formulations based on entrapment of a larvicide in cross-linked carboxymethylcellulose. *Journal of Applied Polymer Science*, *54*(12), 1879–1885.

Puoci, F., Iemma, F., Spizzirri, U. G., Cirillo, G., Curcio, M., & Picci, N. (2008). Polymer in agriculture: A Review. *American Journal of Agricultural and Biological Sciences*, *3*(1), 299–314.

Pasqui, D., Atrei, A., Giani, G., De Cagna, M., & Barbucci, R. (2011). Metal oxide nanoparticles as cross-linkers in polymeric hybrid hydrogels. *Materials Letters*, *65*, 392–395.

Qiu, L., Shao, Z., Wang, D., Wang, F., Wang, W., & Wang, J. (2014). Carboxymethyl cellulose lithium (CMC-Li) as a novel binder and its electrochemical performance in lithium-ion batteries. *Cellulose*, *24*, 2789–2796.

Rabek, J. F. (1980). *Experimental methods in polymer chemistry: Application of wide-angle X-ray diffraction (WAXS) to the study of the structure of polymers*. Chichester: Wiley Interscience.

Rokhade, A. P., Agnihotri, S. A., Patil, S. A., Mallikarjuna, N. N., Kulkarni, P. V., & Aminabhavi, T. M. (2006). Semi-interpenetrating polymer network microspheres of gelatin and sodium carboxymethyl cellulose for controlled release of ketorolac tromethamine. *Carbohydate Polymers*, *65*(3), 243–252.

Rokhade, A. P., Kulkarni, P. V., Mallikarjuna, N. N., & Aminabhavi, T. M. (2009). Preparation and characterization of novel semi-interpenetrating polymer network hydrogel microspheres of chitosan and hydroxypropyl cellulose for controlled release of chlorothiazide. *Journal of Microencapsulation*, *26*(1), 27–36.

Sannino, A., Esposito, A., Rosa, A. D., Cozzolino, A., Ambrosio, L., & Nicolais, L. (2003). Biomedical application of a superabsorbent hydrogel for body water elimination in the treatment of edemas. *Journal of Biomedical Materials Research*, *67*(3), 1016–1024.

Sannino, A., Maffezzoli, A., & Nicolais, L. (2003). Introduction of molecular spacers between the crosslinks of a cellulose-based superabsorbent hydrogel: Effects on the equilibrium sorption properties. *Journal of Applied Polymer Science*, *90*, 168–174.

Sullad, A. G., Manjeshwar, L. S., & Aminabhavi, T. M. (2011). Microspheres of carboxymethyl guar gum for in vitro release of abacavir sulfate: Preparation and Characterization. *Journal of Applied Polymer Science*, *122*, 452–460.

Wang, W., & Wang, F. (2014). Novel functional material carboxymethyl cellulose lithium (CMC-Li) enhanced performance of lithium-ion batteries. *RSC Advances*, *4*(47), 24859–24862.